Masses and Radii of Neutron Stars from Observation and Theory

J. M. Lattimer

Department of Physics & Astronomy
Stony Brook University

and

Yukawa Institute of Theoretical Physics
University of Kyoto

Collaborators: E. Brown (MSU), K. Hebeler (Darmstadt), D. Page (UNAM), C.J. Pethick (NORDITA), M. Prakash (Ohio U), A. Steiner (INT), A. Schwenk (TU Darmstadt), Y. Lim (Daegu Univ., Korea)

Binary Neutron Star Coalescence as a Fundamental Physics Laboratory
Week 3, July 17, 2014, Institute for Nuclear Theory, Seattle

Outline

- General Relativity Constraints on Neutron Star Structure
- The Neutron Star Radius and the Nuclear Symmetry Energy
- Nuclear Experimental Constraints on the Symmetry Energy
- Constraints from Pure Neutron Matter Theory
- Astrophysical Constraints
  - Pulsar and X-ray Binary Mass Measurements
  - Photospheric Radius Expansion Bursts
  - Thermal Emission from Isolated and Quiescent Binary Sources
  - Other Proposed Mass and Radius Constraints

Neutron Star Structure

Tolman-Oppenheimer-Volkov equations

$$\frac{dp}{dr} = -\frac{G}{c^4}\frac{(mc^2 + 4\pi pr^3)(\varepsilon + p)}{r(r - 2Gm/c^2)}$$

$$\frac{dm}{dr} = 4\pi\frac{\varepsilon}{c^2}r^2$$

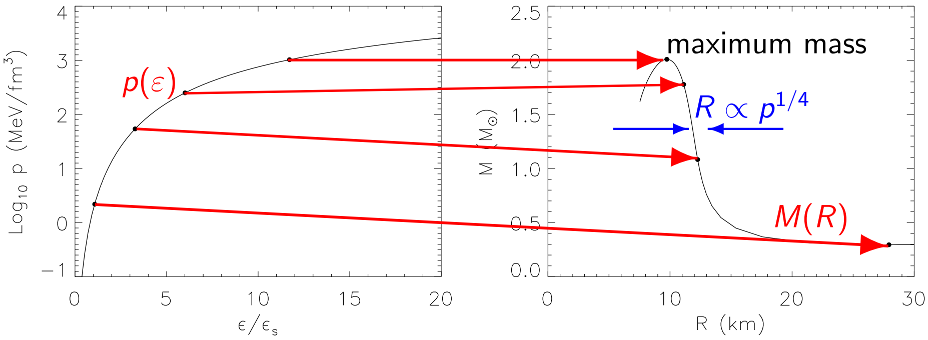

Equation of State ← Observations

Extremal Properties of Neutron Stars

- The most compact and massive configurations occur when the low-density equation of state is "soft" and the high-density equation of state is "stiff" (Koranda, Stergioulas & Friedman 1997).

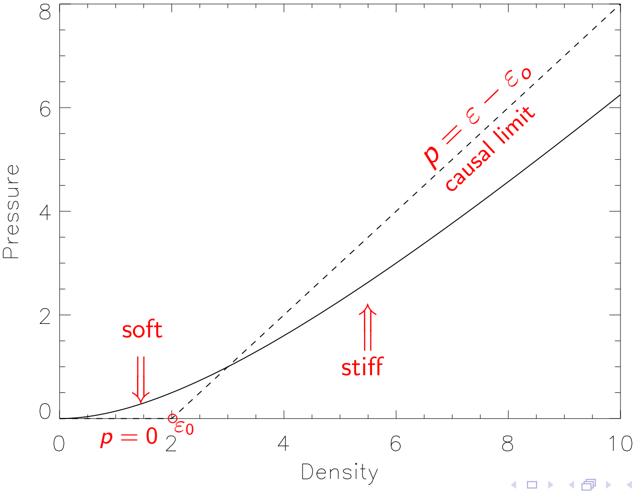

ε_0 is the only EOS parameter

The TOV solutions scale with ε_0

$w = \varepsilon/\varepsilon_0$
$y = p/\varepsilon_0$
$x = r\sqrt{G\varepsilon_0}/c^2$
$z = m\sqrt{G^3\varepsilon_0}/c^2$

Extremal Properties of Neutron Stars

The maximum mass configuration is achieved when
$x_R = 0.2404$, $w_c = 3.034$, $y_c = 2.034$, $z_R = 0.08513$.

A useful reference density is the nuclear saturation density (interior density of normal nuclei):
$\rho_s = 2.7 \times 10^{14}$ g cm^{-3}, $n_s = 0.16$ baryons fm^{-3}, $\varepsilon_s = 150$ MeV fm^{-3}

- $M_{\rm max} = 4.1\ (\varepsilon_s/\varepsilon_0)^{1/2} M_\odot$ (Rhoades & Ruffini 1974)
- $M_{B,\rm max} = 5.41\ (m_B c^2/\mu_o)(\varepsilon_s/\varepsilon_0)^{1/2} M_\odot$
- $R_{\rm min} = 2.82\ GM/c^2 = 4.3\ (M/M_\odot)\ {\rm km}$
- $\mu_{b,\rm max} = 2.09$ GeV
- $\varepsilon_{c,\rm max} = 3.034\ \varepsilon_0 \simeq 51\ (M_\odot/M_{\rm largest})^2\ \varepsilon_s$
- $p_{c,\rm max} = 2.034\ \varepsilon_0 \simeq 34\ (M_\odot/M_{\rm largest})^2\ \varepsilon_s$
- $n_{B,\rm max} \simeq 38\ (M_\odot/M_{\rm largest})^2\ n_s$
- $\mathrm{BE}_{\rm max} = 0.34\ M$
- $P_{\rm min} = 0.74\ (M_\odot/M_{\rm sph})^{1/2}(R_{\rm sph}/10\ {\rm km})^{3/2}\ {\rm ms} = 0.20\ (M_{\rm sph,max}/M_\odot)\ {\rm ms}$

Maximum Energy Density in Neutron Stars

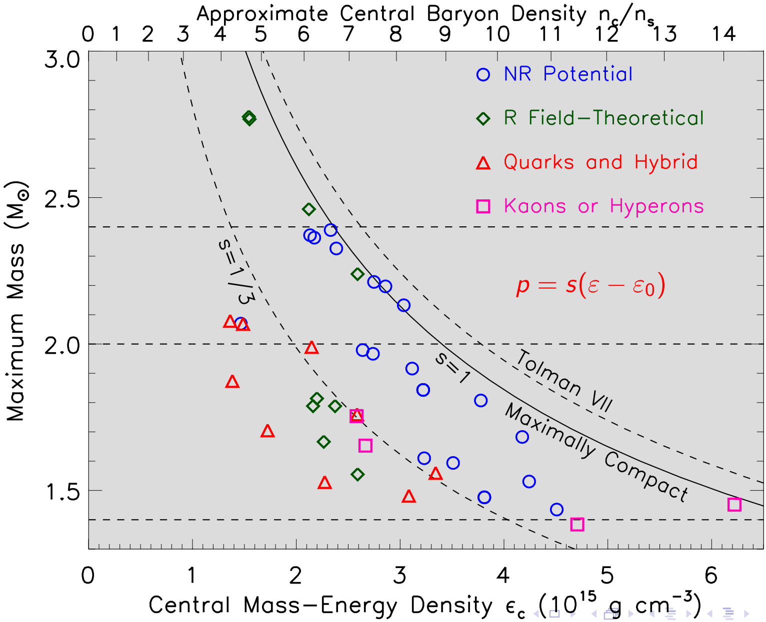

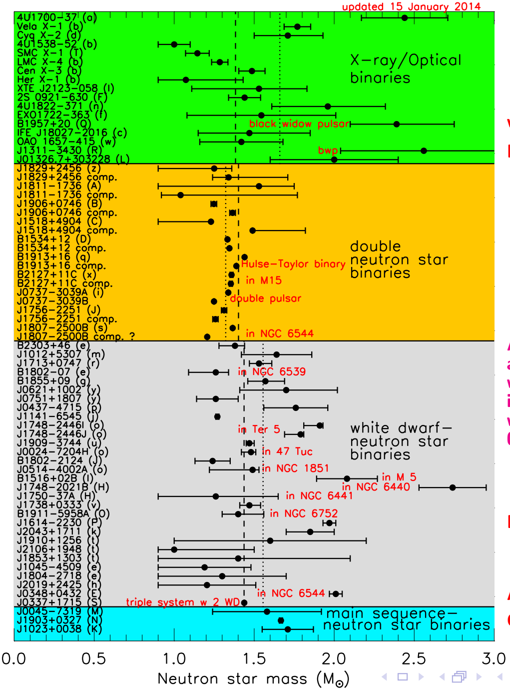

vanKerkwijk 2010

Romani et al. 2012

Although simple average mass of w.d. companions is 0.23 $M_\odot$ larger, weighted average is 0.04 $M_\odot$ smaller

Demorest et al. 2010

Antoniadis et al. 2013

Champion et al. 2008

What is the Maximum Mass?

- PSR J1614+2230 (Demorest et al. 2010) $1.97 \pm 0.04\ M_\odot$
  A nearly edge-on system with well-measured Shapiro time delay
- PSRJ0548+0432 (Antoniadis et al. 2013) $2.01 \pm 0.04\ M_\odot$
  Measured using optical data and theoretical properties of companion white dwarf
- B1957+20 (van Kerkwijk 2010) $2.4 \pm 0.3\ M_\odot$
  Black widow pulsar with $\sim 0.03\ M_\odot$ companion; large mass errors due to uncertainties in tidally-distorted shape of the low-mass companion
- PSR J1311-3430 (Romani et al. 2012) $2.55 \pm 0.50\ M_\odot$
  Another black widow pulsar

Causality + GR Limits and the Maximum Mass

A lower limit to the maximum mass sets a lower limit to the radius for a given mass.

Similarly, a precise (M, R) measurement sets an upper limit to the maximum mass.

$1.4 M_\odot$ stars must have $R > 8.15 M_\odot$.

$1.4 M_\odot$ strange quark matter stars (and likely hybrid quark/hadron stars) must have $R > 11$ km.

$M - R$ curves for maximally compact EOS

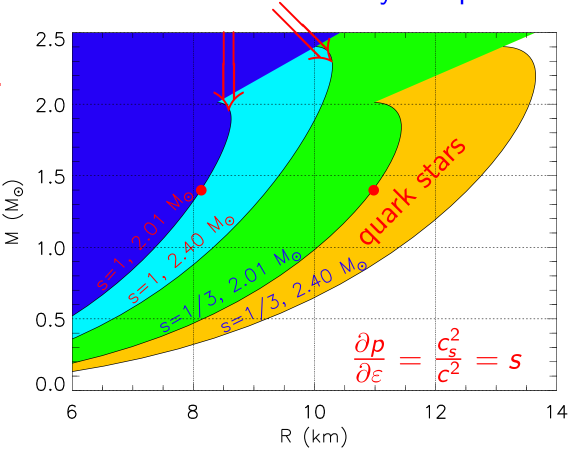

$$\frac{\partial p}{\partial \varepsilon} = \frac{c_s^2}{c^2} = s$$

Mass-Radius Diagram and Theoretical Constraints

GR:
$R > 2GM/c^2$

$P < \infty$:
$R > (9/4)GM/c^2$

causality:
$R \gtrsim 2.9GM/c^2$

— normal NS
— SQS

— $R_\infty = \frac{R}{\sqrt{1-2GM/Rc^2}}$

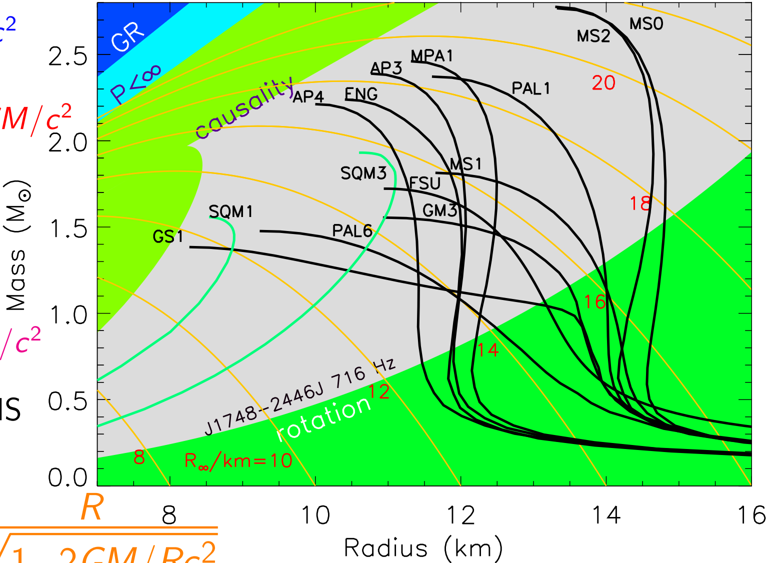

The Radius – Pressure Correlation

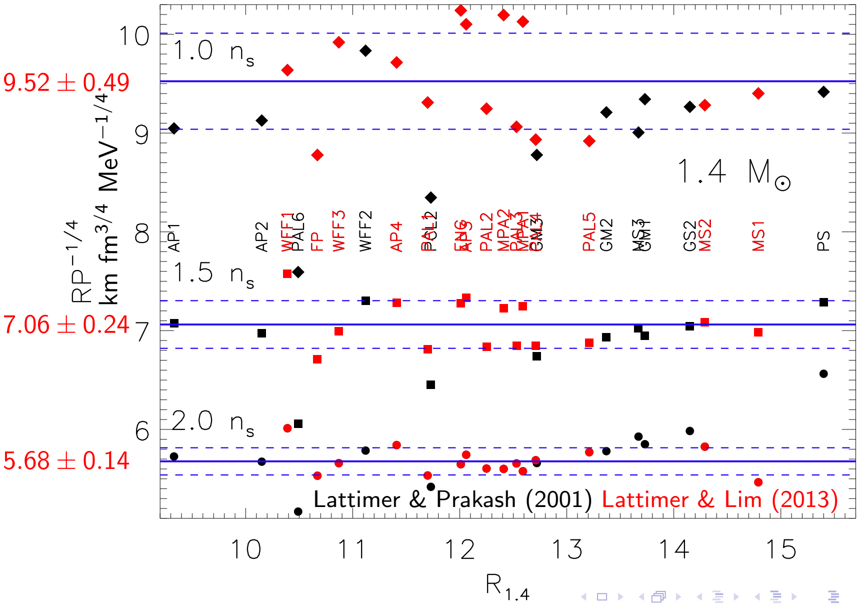

Nuclear Symmetry Energy

Defined as the difference between energies of pure neutron matter ($x = 0$) and symmetric ($x = 1/2$) nuclear matter.

$$S(\rho) = E(\rho, x = 0) - E(\rho, x = 1/2)$$

Expanding around the saturation density (ρ_s) and symmetric matter ($x = 1/2$)

$$E(\rho, x) = E(\rho, 1/2) + (1-2x)^2 S_2(\rho) + \dots$$

$$S_2(\rho) = \mathbf{S_v} + \frac{\mathbf{L}}{3}\frac{\rho - \rho_s}{\rho_s} + \dots$$

$$\mathbf{S_v} \simeq 31 \text{ MeV}, \quad \mathbf{L} \simeq 50 \text{ MeV}$$

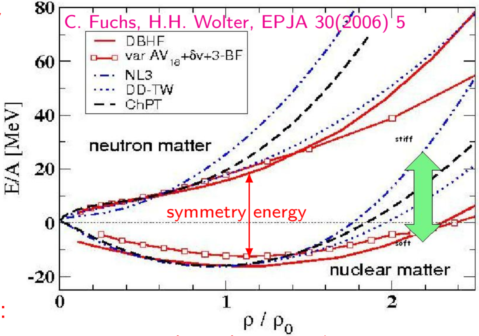

Connections to pure neutron matter:

$$E(\rho_s, 0) \approx S_v + E(\rho_s, 1/2) \equiv S_v - B, \qquad p(\rho_s, 0) = L\rho_s/3$$

Neutron star matter (in beta equilibrium):

$$\frac{\partial(E + E_e)}{\partial x} = 0, \quad p(\rho_s, x_\beta) \simeq \frac{L\rho_s}{3}\left[1 - \left(\frac{4S_v}{\hbar c}\right)^3 \frac{4 - 3S_v/L}{3\pi^2\rho_s}\right]$$

Nuclear Experimental Constraints

Binding Energies

Liquid Droplet Model

$$E_{sym} = AI^2\left[\frac{S_v}{1+S_sA^{-1/3}/S_v} - \frac{Ze^2}{20R}\frac{S_sA^{-1/3}/S_v}{1+S_sA^{-1/3}/S_v}\right]$$

$$\frac{S_s}{S_v} \simeq \frac{3a}{2r_o}\left[1+\frac{L}{3S_v}+\left(\frac{L}{3S_v}\right)^2\cdots\right]$$

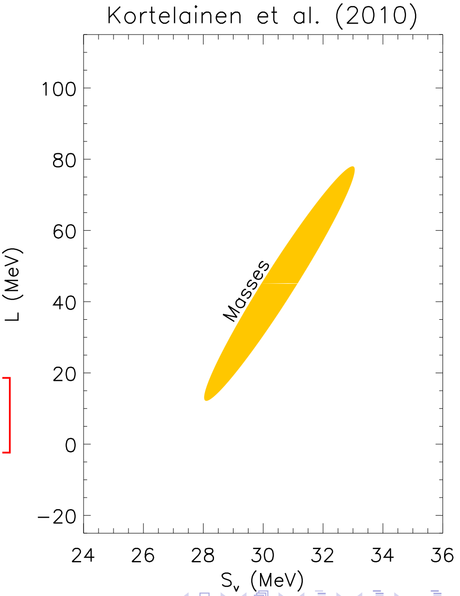

Nuclear Experimental Constraints

Neutron Skin Thicknesses

$$r_{np} = \frac{2r_o}{3S_v}\frac{1}{\sqrt{1-I^2}}\left(1+S_sA^{-1/3}/S_v\right)^{-1}$$
$$\times\sqrt{\frac{3}{5}}\left[IS_s - \frac{3Ze^2}{140r_o}\left(1+\frac{10}{3}\frac{S_sA^{-1/3}}{S_v}\right)\right]$$

$$r_{np,208} = 0.175 \pm 0.020 \text{ fm}$$

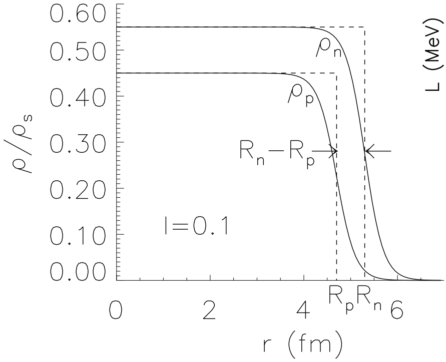

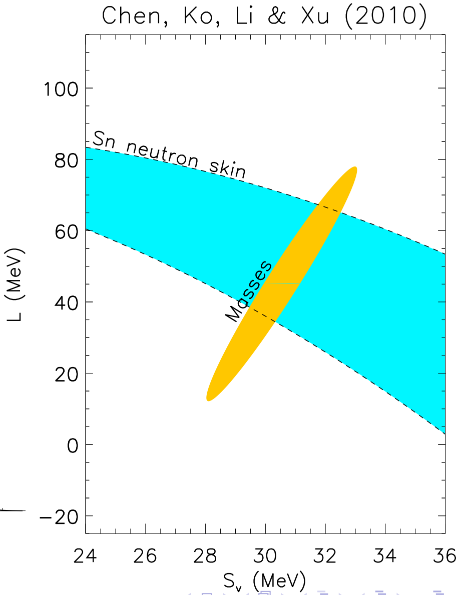

Nuclear Experimental Constraints

Flows in
Heavy Ion Collisions

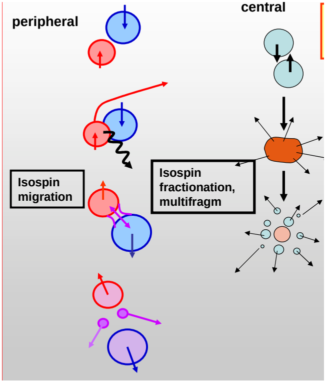

Wolter, NuSYM11

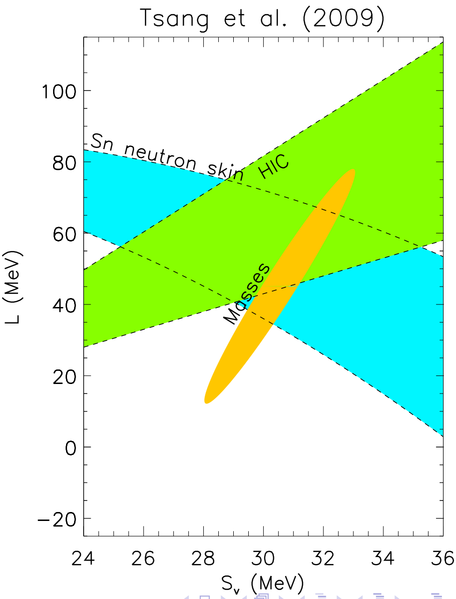

Nuclear Experimental Constraints

Giant Dipole Resonance Centroids

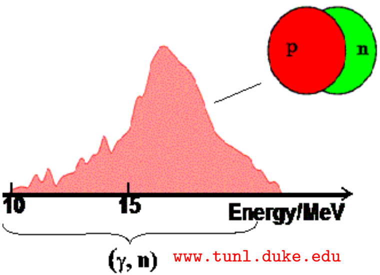

23.3 MeV$< S_2(0.1\ \mathrm{fm}^{-3}) <$24.9 MeV

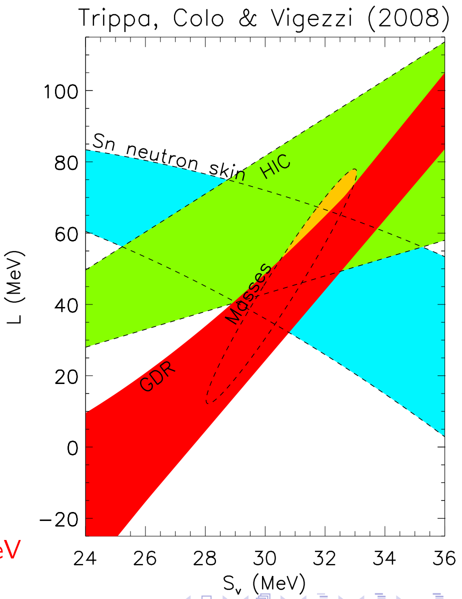

Nuclear Experimental Constraints

Dipole Polarizabilities

$$\alpha_D = 4m_{-1}$$

$$\simeq \frac{AR^2}{20S_v}\left(1 + \frac{5}{3}\frac{S_s A^{-1/3}}{S_v}\right)$$

Uses data of
Tamii et al. (2011)

$$\alpha_{D,208} = 20.1 \pm 0.6 \text{ fm}^2$$

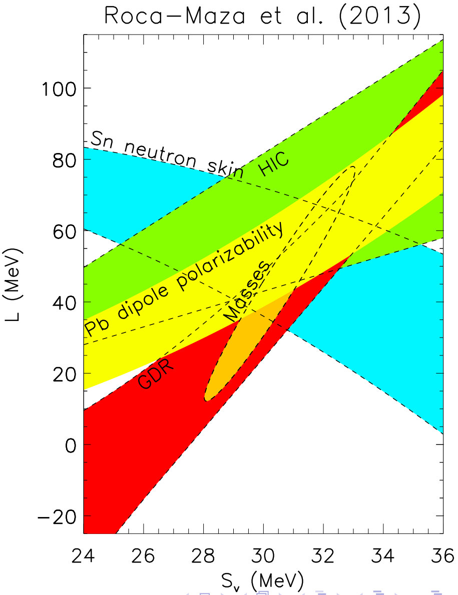

Nuclear Experimental Constraints

Isobaric Analog States

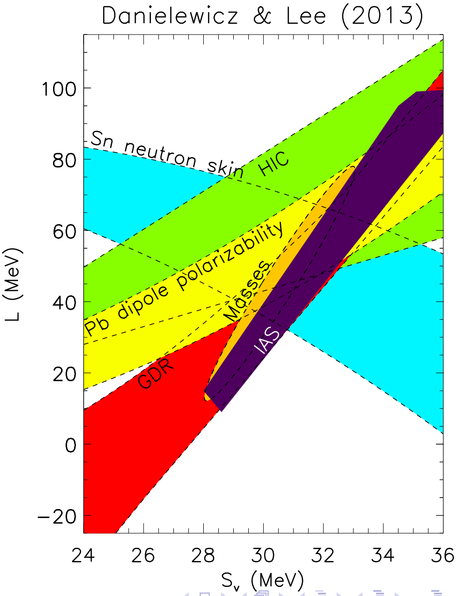

Theoretical Neutron Matter Calculations

H&S: Chiral Lagrangian

GC&R: Quantum Monte Carlo

$S_v - L$ constraints from Hebeler et al. (2012)

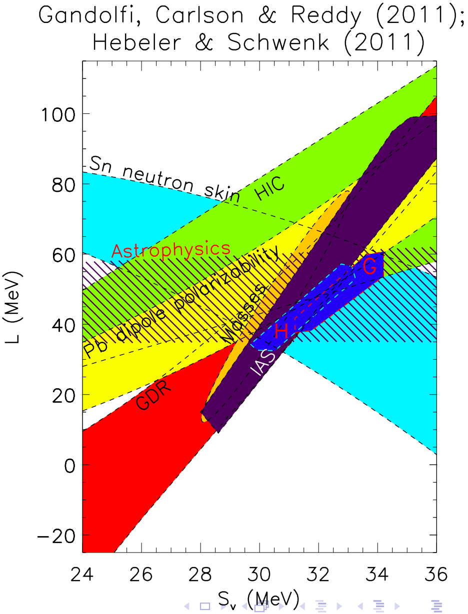

Theoretical Neutron-Rich Matter Calculations

The usual assumption is that the symmetry energy $S(n)$ is sufficiently well approximated by the quadratic expression

$$E_{sym}(n,x) \simeq S_2(n)\,(1-2x)^2\,.$$

But chiral Lagrangian studies of neutron and neutron-rich matter by Drischler, Somá & Schwenk (2014) indicate the presence of quartic or higher contributions

$$E_{sym}(n,x) \simeq S_2(n)\,(1-2x)^2 + S_4(n)\,(1-2x)^4 + \cdots\,.$$

Theoretical results fitted with model energy having possible quartic parameters α and β:

$$\begin{aligned}
\frac{E(n,x)}{T_0} &= \frac{3}{5}(2u)^{2/3}\Big[\left(x^{5/3}+(1-x)^{5/3}\right)(1+bu) \\
&+ (a-b)u\left(x^{8/3}+(1-x)^{8/3}\right)\Big] \\
&- u\left[\frac{\alpha}{2}+\left(\alpha_L-\frac{\alpha}{2}\right)(1-2x)^2+\beta(1-2x)^4\right] \\
&+ u^\gamma\left[\frac{\eta}{2}+\left(\eta_L-\frac{\eta}{2}\right)(1-2x)^2+\delta(1-2x)^4\right].
\end{aligned}$$

Fits to Neutron-Rich Matter

Drishler, Somá & Schwenk (2014)

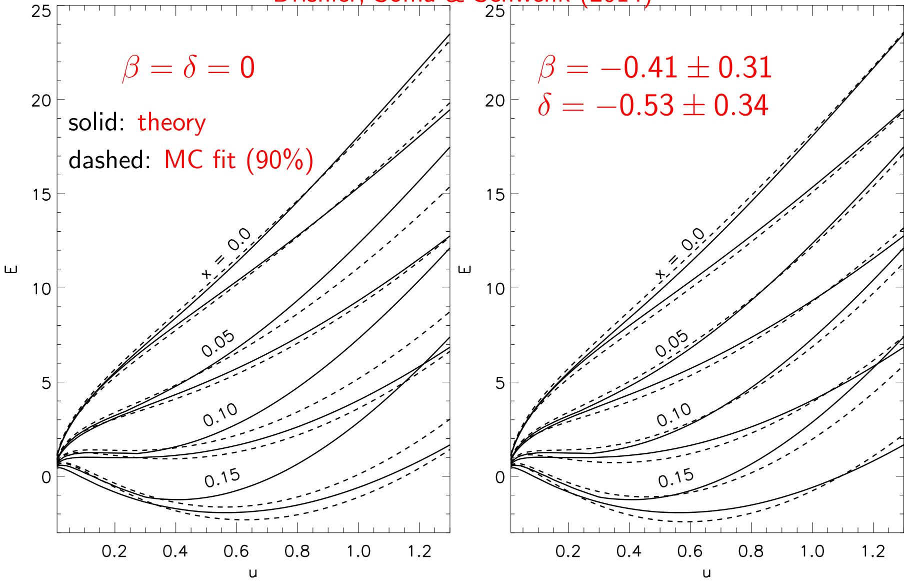

Fits to Neutron-Rich Matter

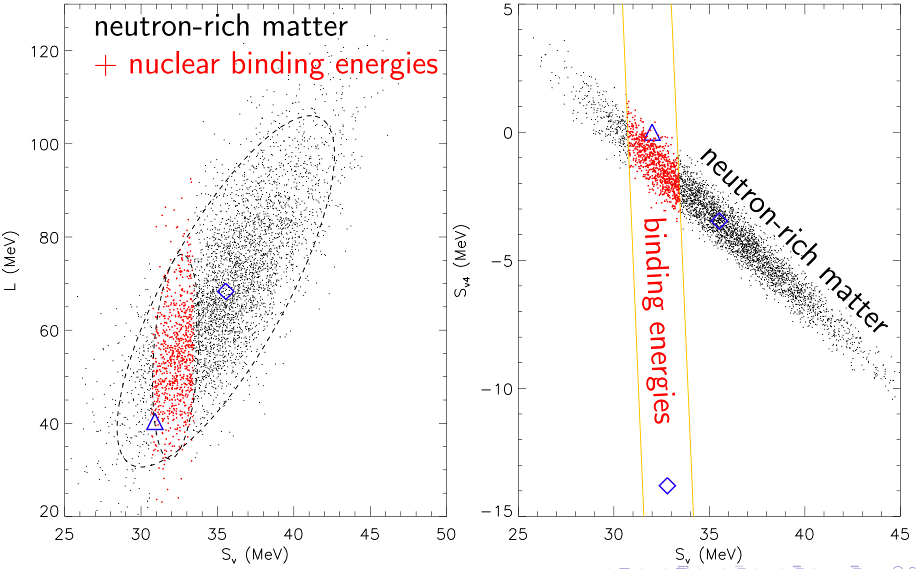

Theoretical Neutron-Rich Matter Calculations

Chiral Lagrangian studies of neutron and neutron-rich matter by Drischler, Somá & Schwenk (2014)

Interpreted by Lattimer (2014)

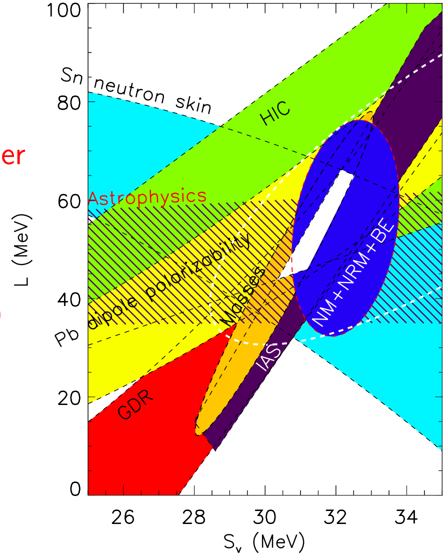

Simultaneous Mass/Radius Measurements

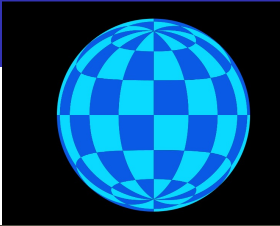

- Measurements of flux $F_\infty = (R_\infty/D)^2 \sigma T_{\rm eff}^4$ and color temperature $T_c \propto \lambda_{\rm max}^{-1}$ yield an apparent angular size (pseudo-BB):

$$\frac{R_\infty}{D} = \frac{R}{D}\frac{1}{\sqrt{1-2GM/Rc^2}}$$

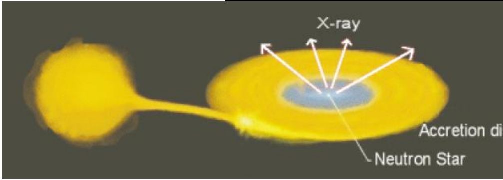

- Observational uncertainties include distance D, interstellar absorption N_H, atmospheric composition

Best chances for accurate radius measurement:

- Nearby isolated neutron stars with parallax (uncertain atmosphere)
- Quiescent low-mass X-ray binaries (QLMXBs) in globular clusters (reliable distances, low B H-atmosperes)
- Bursting sources (XRBs) with peak fluxes close to Eddington limit (where gravity balances radiation pressure)

$$F_{\rm Edd} = \frac{cGM}{\kappa D^2}\sqrt{1-2GM/Rc^2}$$

$M - R$ PRE Burst Estimates

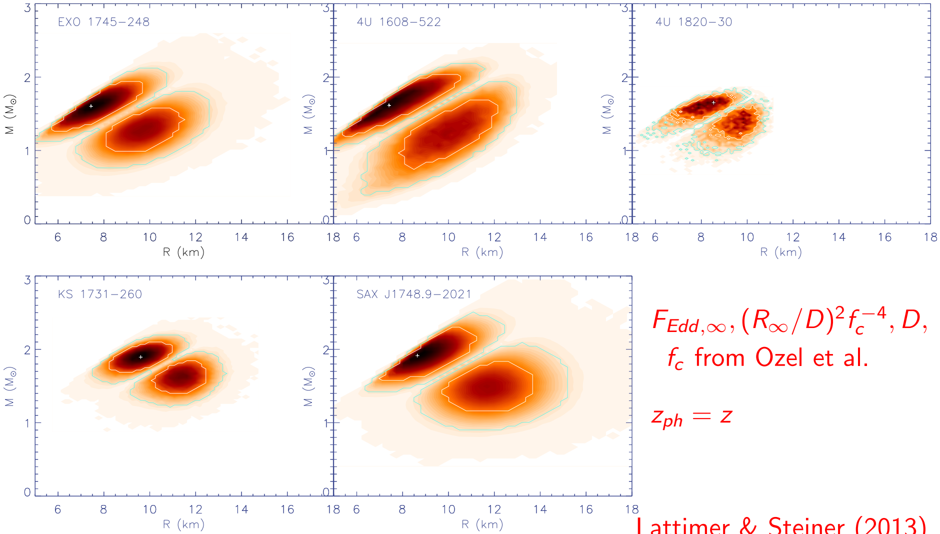

$F_{Edd,\infty}, (R_\infty/D)^2 f_c^{-4}, D,$ f_c from Ozel et al.

$z_{ph} = z$

Lattimer & Steiner (2013)

$M - R$ PRE Burst Estimates

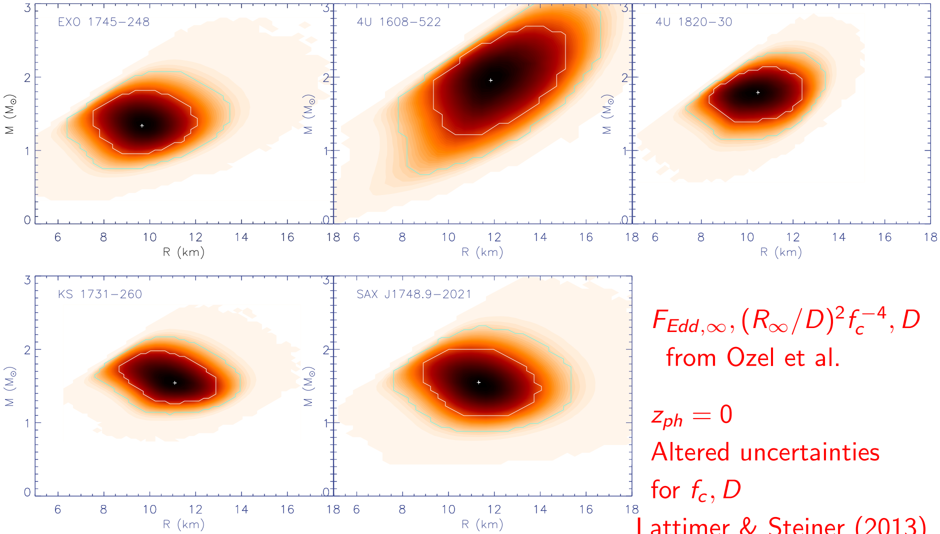

$F_{Edd,\infty}, (R_\infty/D)^2 f_c^{-4}, D$ from Ozel et al.

$z_{ph} = 0$

Altered uncertainties for f_c, D

Lattimer & Steiner (2013)

$M - R$ QLMXB Estimates

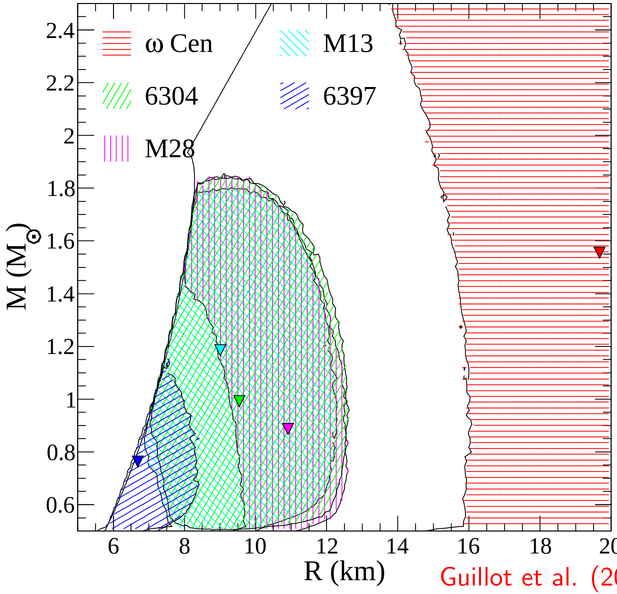

Absorption (N_H) determined self-consistently from spectra

Guillot et al. (2013)

$M - R$ QLMXB Estimates

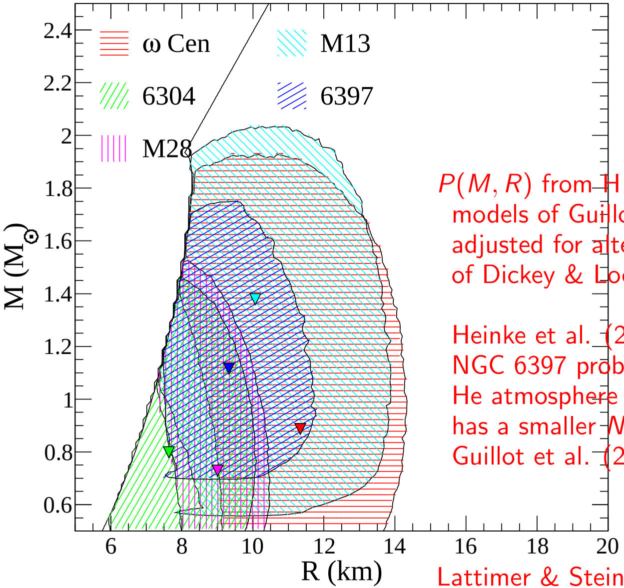

$P(M, R)$ from H atmosphere models of Guillot et al. (2013), adjusted for alternate N_H values of Dickey & Lockman (1990).

Heinke et al. (2014) found NGC 6397 probably has a He atmosphere and ω Cen has a smaller N_H than Guillot et al. (2013) found.

Lattimer & Steiner (2013)

Bayesian TOV Inversion

- $\varepsilon < 0.5\varepsilon_0$: Known crustal EOS
- $0.5\varepsilon_0 < \varepsilon < \varepsilon_1$: EOS parametrized by K, K', S_v, γ
- Polytropic EOS: $\varepsilon_1 < \varepsilon < \varepsilon_2$: n_1; $\varepsilon > \varepsilon_2$: n_2

- EOS parameters $K, K', S_v, \gamma, \varepsilon_1, n_1, \varepsilon_2, n_2$ uniformly distributed
- $M_{\rm max} \geq 1.97$ M$_\odot$, causality enforced
- All 10 stars equally weighted

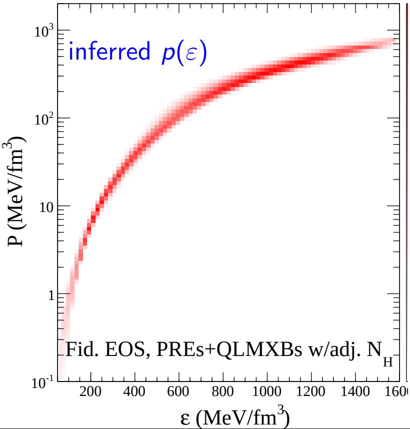

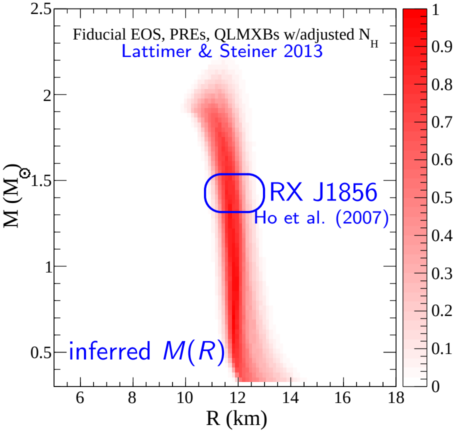

Astronomy vs. Astronomy vs. Physics

Ozel et al., PRE bursts $z_{\rm ph}$ z: $R = 9.74 \pm 0.50$ km.

Suleimanov et al., long PRE bursts: $R_{1.4} \gtrsim 13.9$ km

Guillot et al. (2013), all stars have the same radius, self N_H: $R = 9.1^{+1.3}_{-1.5}$ km.

Lattimer & Steiner (2013), TOV, crust EOS, causality, maximum mass $> 2M_\odot$, $z_{\rm ph} = z$, alt N_H.

Lattimer & Lim (2013), nuclear experiments: 29 MeV $< S_v <$ 33 MeV, 40 MeV $< L <$ 65 MeV, $R_{1.4} = 12.0 \pm 1.4$ km.

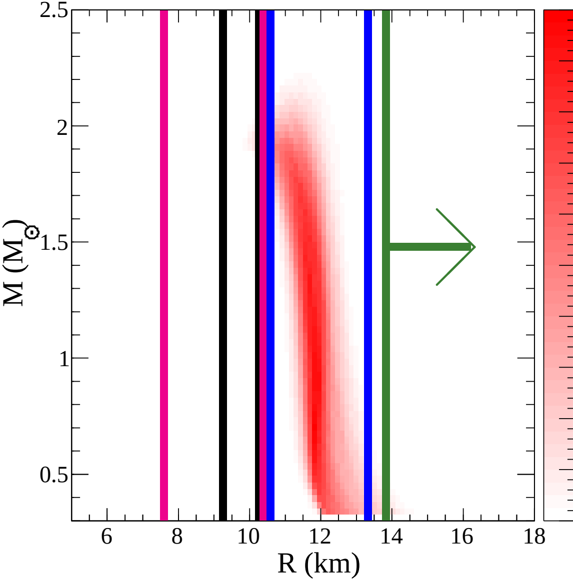

Can Hyperons Appear in Abundance in Neutron Stars?

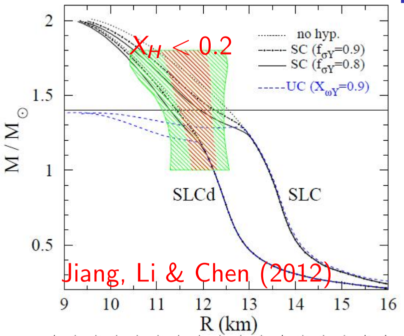

Jiang, Li & Chen (2012)

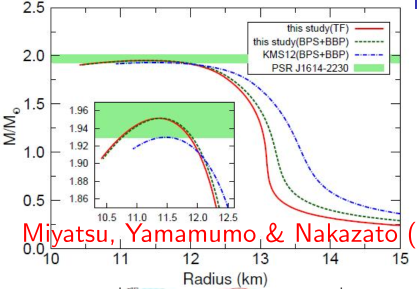

Miyatsu, Yamamumo & Nakazato (2013)

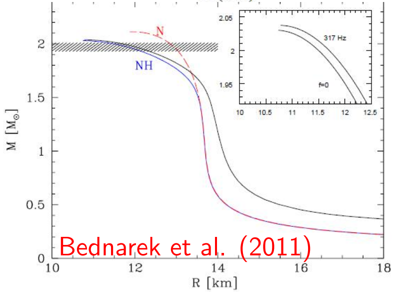

Bednarek et al. (2011)

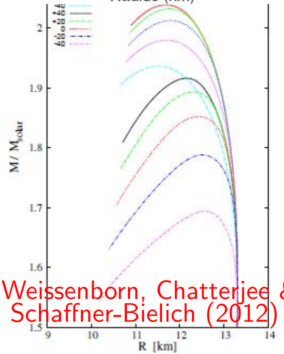

Weissenborn, Chatterjee & Schaffner-Bielich (2012)

Hyperon Stars with Small Radii

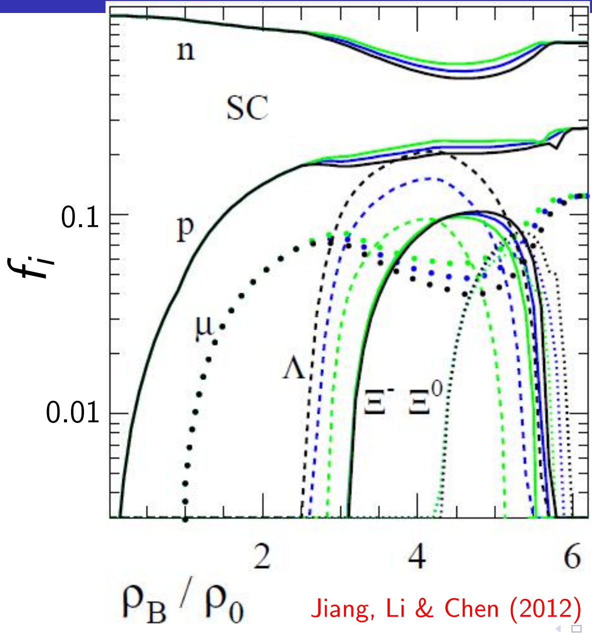

Jiang, Li & Chen (2012)

More Hyperon Stars

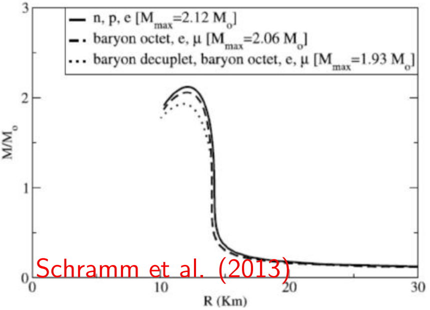

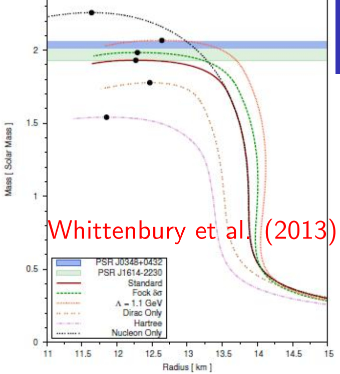

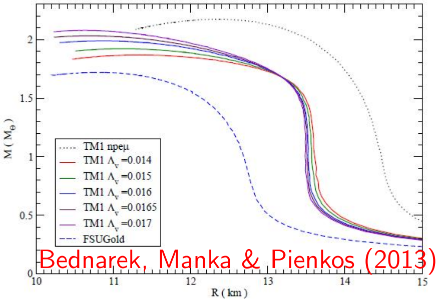

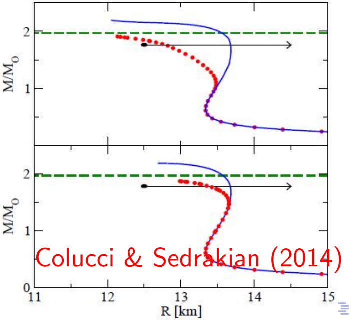

Still More Hyperon Stars

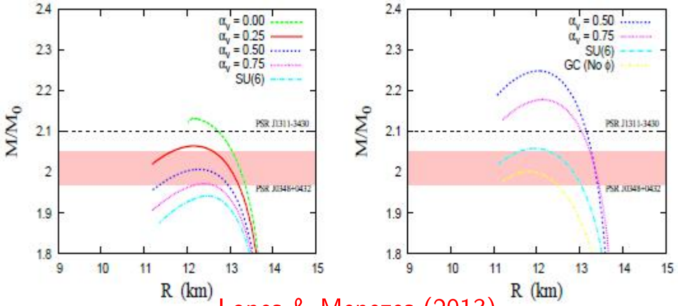

Lopes & Menezes (2013)

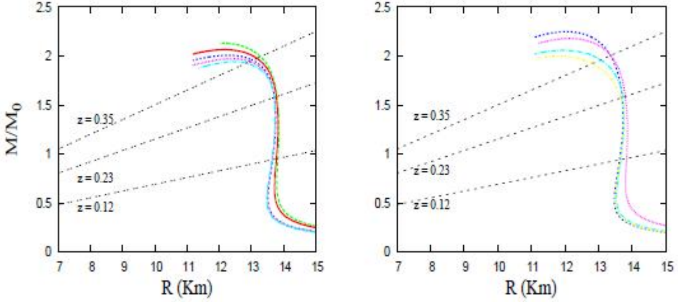

Another Approach – Hadron-Quark Crossover

Replace phase transition with ad-hoc crossover (physical justification?)

$P(\rho) = P_H f_-(\rho) + P_Q f_+(\rho)$

$f_\pm(\rho) = [1 \pm \tanh\{(\rho - \bar{\rho})/\Gamma)\}]/2$

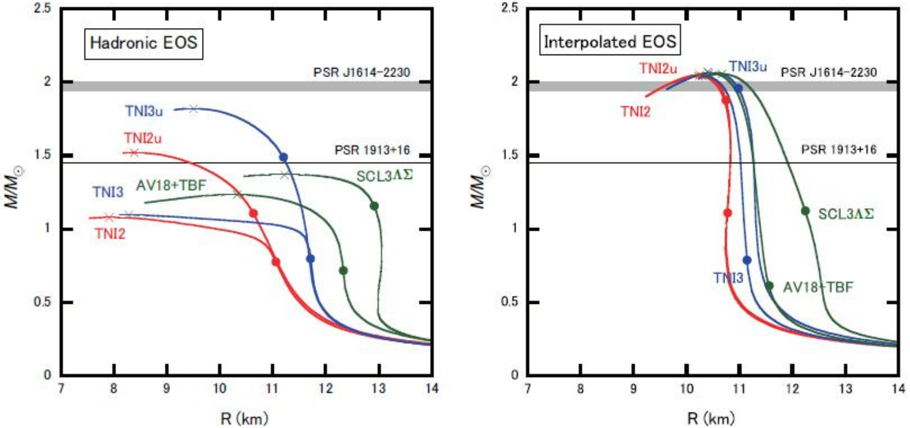

Masuda, Hatsuda & Takatsuka (2012)

Additional Proposed Radius and Mass Constraints

- **Pulse profiles**
  Hot or cold regions on rotating neutron stars alter pulse shapes: NICER and LOFT will enable timing and spectroscopy of thermal and non-thermal emissions. Light curve modeling $\rightarrow M/R$; phase-resolved spectroscopy $\rightarrow R$.
- **Moment of inertia**
  Spin-orbit coupling of ultra-relativistic binary pulsars (e.g., PSR 0737+3039) vary i and contribute to $\dot{\omega}$: $I \propto MR^2$.
- **Supernova neutrinos**
  Millions of neutrinos detected from a Galactic supernova will measure BE$= m_B N - M$, $< E_\nu >$, τ_ν.
- **QPOs from accreting sources**
  ISCO and crustal oscillations

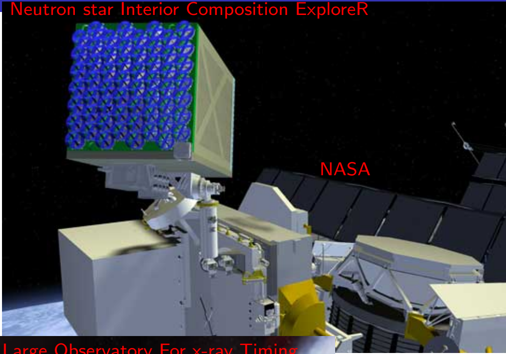

Constraints from Observations of Gravitational Radiation

Mergers:

Chirp mass $\mathcal{M} = (M_1 M_2)^{3/5} M^{-1/5}$ and tidal deformability $\lambda \propto R^5$ (Love number) are potentially measurable during inspiral.

$\bar{\lambda} \equiv \lambda M^{-5}$ is related to $\bar{I} \equiv I M^{-3}$ by an EOS-independent relation (Yagi & Yunes 2013). Both $\bar{\lambda}$ and $\bar{I}$ are also related to M/R in a relatively EOS-independent way (Lattimer & Lim 2013).

- Neutron star - neutron star: $M_{\rm crit}$ for prompt black hole formation, $f_{\rm peak}$ depends on R.
- Black hole - neutron star: $f_{\rm tidal\ disruption}$ depends on $R, a, M_{\rm BH}$. Disc mass depends on $a/M_{\rm BH}$ and on $M_{\rm NS} M_{\rm BH} R^{-2}$.

Rotating neutron stars: r-modes

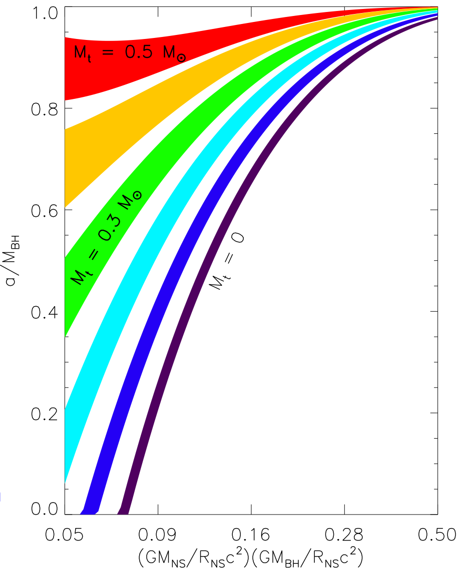

Conclusions

- Nuclear experiments set reasonably tight constraints on symmetry energy parameters and the symmetry energy behavior near the nuclear saturation density.
- Theoretical calculations of pure neutron matter predict very similar symmetry constraints.
- These constraints predict neutron star radii $R_{1.4}$ in the range 12.0 ± 1.4 km.
- Combined astronomical observations of photospheric radius expansion X-ray bursts and quiescent sources in globular clusters suggest $R_{1.4} \sim 12.1 \pm 0.6$ km.
- The nearby isolated neutron star RX J1856-3754 appears to have a radius near 12 km, assuming a solid surface with thin H atmosphere (Ho et al. 2007).
- The observation of a 1.97 $M_\odot$ neutron star, together with the radius constraints, implies the EOS above the saturation density is relatively stiff; abundance of hyperons or any phase transition must be small.

Consistency with Neutron Matter and Heavy-Ion Collisions